Environmental Science
Processes & Impacts

PAPER

View Article Online
View Journal | View Issue

Cite this: *Environ. Sci.: Processes Impacts*, 2015, **17**, 370

Mineralization pathways of organic matter deposited in a river–lake transition of the Rhone River Delta, Lake Geneva

Marie-Eve Randlett,[ab] Sebastien Sollberger,[ab] Tonya Del Sontro,[ab] Beat Müller,[a] Juan Pablo Corella,[c] Bernhard Wehrli[ab] and Carsten J. Schubert*[a]

Received 29th August 2014
Accepted 25th November 2014

DOI: 10.1039/c4em00470a

rsc.li/process-impacts

During the éLEMO endeavour (a research project in which the Russian MIR submersibles were used for studying Lake Geneva) four sediment cores were retrieved on a transect from the delta of the Rhone River towards the profundal part of the lake. The degradation pathways of organic material (OM) were investigated considering different electron acceptors. Essentially, OM at the delta sites had a higher fraction of terrestrial material than the lake sites indicated by higher C/N ratios, and higher long-chain *n*-alkane and alcohol concentrations. The concentrations of chlorins were higher at the distant sites indicating more easily degradable OM in the sediments. However, the chlorin index that was used to determine the degradation state of the OM material indicated that pigment derived OM of deltaic sediments was less degraded than that of the profundal sediments. The fluxes of reduced species from the sediments decreased from the delta to the profundal for CH_4 (from 2.3 to 0.5 mmol m^{-2} d^{-1}) and NH_4^+ (from 0.31 to 0.13 mmol m^{-2} d^{-1}). Fluxes of Fe(II) and Mn(II), however, increased although they were generally very low (between 9×10^{-5} and 7.6×10^{-3} mmol m^{-2} d^{-1}). Oxygen concentration profiles in the pore waters revealed lower fluxes close to the river inflow with 4.3 and 4.1 mmol m^{-2} d^{-1} compared to two times higher fluxes at the profundal sites (8.8 and 8.2 mmol m^{-2} d^{-1}). The rates for totally mineralized OM (R_{total}) at the shallower sites (4.7 mmol C m^{-2} d^{-1}) were only half of those of the deeper sites (9.7 mmol C m^{-2} d^{-1}). Accordingly, not only the rates but also the mineralization pathways differed between the shallow and profundal sites. Whereas only 0–6% of the OM was mineralized aerobically at the shallow sites (since almost all O_2 was used to oxidize the large flux of CH_4 from below) the situation was reversed at the deeper sites and the fraction of aerobically degraded OM was 72–78%. We found a better efficiency in CH_4 production per carbon equivalent deposited at the deeper sites as a result of the higher degradability of the mainly autochthonous OM in spite of the lower deposition rate and the higher degradation state of the OM compared to the delta sites.

Environmental impact

Although lakes cover only 2–3% of the earth's surface they contribute up to 16% of all natural global methane emissions. We studied organic matter degradation and subsequent methane emission from the delta and profundal part of Lake Geneva. Early diagenetic processes were traced and quantified from pore water concentration gradients of various electron acceptors (oxygen, nitrate, Fe, and Mn) and methane production was measured. 72–78% of the OC was mineralized aerobically at the deeper sites but only 0–6% at the shallow sites leading to higher CH_4 production per sedimented OC and higher methane fluxes. Hence, at deltas high methane emissions are expected in lacustrine systems, whereas in the deeper more central parts little methane is produced and hardly reaches the atmosphere.

1 Introduction

Whereas countless studies on the transformation of organic material (OM) during degradation have been performed in the marine environment,[1–3] studies in lakes on the same topic are rather rare.[4,5] The understanding of preservation of OM that has been formed during photosynthesis and subsequently has been moved to and buried into the sediments is crucial for at least two reasons: first, we need to understand how OM is preserved

[a]*Eawag, Swiss Federal Institute of Aquatic Science and Technology, 6047 Kastanienbaum, Switzerland. E-mail: carsten.schubert@eawag.ch*
[b]*ETH, Swiss Federal Institute of Technology, Institute of Biogeochemistry and Pollutant Dynamics, 8092 Zurich, Switzerland*
[c]*Museo Nacional de Ciencias Naturales (MNCN/CSIC), Serrano 115bis, 28006 Madrid, Spain*

† Electronic supplementary information (ESI) available. See DOI: 10.1039/c4em00470a

or degraded on its way to the formation of oil or gas depending on the environment and redox conditions during burial/diagenesis. Second, and this might be a more important question at this moment of time, how much of the aquatic OM primarily built from atmospheric carbon dioxide (CO_2) is finally buried in the sediments. The increase of CO_2 and methane (CH_4) in the atmosphere since the last ice age and, even more dramatically, over the last 150 years[6–8] is naturally balanced only (*i.e.*, not considering man made possibilities like carbon storage in the ocean or deeper terrestrial environments) by the uptake of CO_2 by oceans/lakes and/or terrestrial biomass. The fixation of CO_2 in the biomass and the subsequent burial in soils and sediments diminishes CO_2 concentrations in the atmosphere and hence is crucial to understand the conditions that eventually decide about either mineralization or burial of OM. The burial efficiency of OM in lakes was highlighted recently.[4] These authors found high organic carbon (OC) burial efficiency (ratio between OC buried to OC deposited) in lakes in general (0.48) and especially in lakes influenced by a high allochthonous input. A previous study estimated the OC buried in lake sediments to be 50% of what is stored in the ocean[9] which is a huge number when comparing the ocean area (71%) to the integrated global lake area (2–3%).[10] In addition to the fact that sediments receiving a high input of suspended particulate matter have high OC burial efficiencies a closely linked factor was the oxygen (O_2) exposure time.[4] However, it is not only O_2 that is used as an electron acceptor when OC is degraded but also other oxidants like nitrate, iron, manganese, and sulfate can play a substantial role.[11] In a study of the meromictic Lake Zug, sediments in which the input of allochthonous material can be neglected the distinction between aerobic and anaerobic degradation of OM showed that in the shallower part of the lake with oxic bottom water around 50% of the OM was degraded with O_2.[12] Hence, it is important to consider other electron acceptors besides O_2 that might play a role in OM degradation. The study presented here focuses on the diagenetic degradation pathways and the factors controlling the burial efficiency of OM in Lake Geneva sediments. Lipids and pigments were studied in the sediments as indicators of the origin of sediment OM and electron acceptors in the sediment pore waters when moving from the delta of the main tributary, the Rhone River (higher river inflow, deltaic sites) to the deeper part of the lake (less river influence, profundal sites).

2 Materials and methods

2.1 Sampling site

Lake Geneva is the largest western European lake with a surface area of 582 km^2, a volume of 89 km^3 and a maximum depth of 309 m. With a catchment area of 5220 km^2, the Rhone River makes up 68% of the input to the lake.[13] The annual discharge ranged between 127 and 227 $m^3\ s^{-1}$ for the period 1935–2008.[14] The annual sediment load transported by the Rhone River into Lake Geneva varies between 2 and 9 $\times$ 10^6 tonnes per year[15] providing large amounts of allochthonous OM supply mainly to the large delta.

2.2 Sampling

Sediment cores and peeper samples[16] were collected at 4 locations from the northeastern part of Lake Geneva in front of the inflow of the Rhone River with increasing distance from the shore using the MIR submersibles[17] and piston cores from a boat (Fig. 1 ESI;† Table 1). For each site, 3 sediment cores (inner diameter = 59 mm) were collected: one for CH_4 analysis, one for porosity and bulk parameters and one for biomarker analysis. Sediment cores were sliced in 1 cm sections, frozen and freeze dried. Pore water equilibrators (peepers;[18,19]) were used and consisted of a 50 $\times$ 15 cm solid, plexiglass frame into which cells (1.5 $\times$ 3 cm) were milled at a spacing of either 0.5 or 1.5 cm. The cells were filled with distilled, deionized water, and a 0.2 μm filter (HT 200, Tuffryn polysulfone membrane; Gelman Inc.) was laid over the surface of the frame and held in place by an outer frame of plexiglass.[16] To remove O_2 from the water in the cells, the peeper was immersed in a tank of deionized water that was then purged for 24 hours with nitrogen.[20] When the peeper is placed in the sediments, solutes from pore water in contact with the filter diffuse into the cells such that, after equilibrium is reached, concentrations inside each cell equal those at the corresponding depth in the pore water. A one week period was allowed for equilibration which allows *e.g.* over 90% of sulfate (which has a low diffusion coefficient) to be equilibrated (after 5.6 days; a more than 99% equilibration would need about 130 days;[19]). Peepers were mounted on a steel tripod that was positioned on the sediment surface. Exposure of the peeper to lake water following retrieval from the sediments was minimized and lasted no more than 3–5 minutes. Sampling of the cells was done immediately upon retrieval within less than an hour (preferable between 15 and 30 min) after recovery. Water from within the cells was sampled with pipettes and immediately transferred into vials containing appropriate fixative agents (see below for different species).

2.3 Sedimentation rates

To determine sedimentation rates (SRs) in the profundal area, core #5 was dated by gamma spectrometry using ^{137}Cs on freeze-dried and ground sediment with a HPGe detector (Canberra GCW-3523) using an energy of 661.7 keV. SRs and accumulation rates (ARs) were calculated based on the ^{137}Cs peaks from the Chernobyl accident and nuclear bomb tests assuming a constant rate of supply (CRS) according to the model of Niessen and Appleby.[21,22] The SR of core #4, was estimated by correlation using the TOC profile with the nearby core #5 (see Fig. 2A, ESI†). Since cores #1 and #2 could not be dated through neither ^{210}Pb nor ^{137}Cs due to low activities we correlated the cores *via* the TOC profile to the nearby core LP (ESI Fig. 1,† N 46°24.190′; E 6°50.493) from 103 m water depth which was ^{14}C and ^{137}Cs dated (see Fig. 2B, ESI,† *c.f.*[23]).

2.4 Bulk parameters

Total carbon (TC) and total nitrogen (TN) were measured in freeze-dried samples with a Thermo Quest CE Instrument NC 2500. Total organic carbon (TOC) was measured on decalcified

Table 1 Dates when cores were taken. Coordinates, water depths, and sediment depths of the studied cores. TOC concentration, sedimentation rates (SRs), porosity, and accumulation rates (ARs) of the analysed sediment cores. TOC concentrations and porosity were averaged below 3 cm and over the uppermost 9 cm, respectively. Efficiency describes the CH_4 produced per g deposited carbon

	Date	Coordinates		Water depth	Sed. depth	TOC	Sed. rate (SR)		Accumulation rate AR		Efficiency
Site #	dd.m.yy	WGS 84		m	cm	%	cm per year	Porosity	kg m^{-2} per year	gC m^{-2} per year	mmol CH_4 per gC
1	17.6.13	N 46°24.416′	E 6°50.667′	130	21	0.43	2.3	0.57	26.8	131.7	5.4
2	17.6.13	N 46°24.321′	E 6°50.975′	90	44	0.45	2.3	0.53	28.1	129.8	6.6
4	14.7.13	N 46°26.231′	E 6°49.364′	210	27	0.74	0.6	0.75	4.1	31.2	8.1
5	14.7.13	N 46°27.048′	E 6°47.933′	240	30	0.83	0.4	0.77	2.4	19.8	9.1

samples.[24] In brief, sediment samples were acid treated with 10% HCl until no further CO_2 evolved and dried at 40 °C before weighing for elemental analysis. Total inorganic carbon (TIC) was calculated as the difference between TC and TOC. The precision for TC and TOC was ±0.1 wt% and ±0.2 wt% for TN. $\delta^{13}C$ and $\delta^{15}N$ of the OM were obtained with a GV Instruments IsoPrime isotope ratio mass spectrometer (IRMS). The precision of $\delta^{13}C$ in ‰ *vs.* Vienna Peedee Belemnite (VPDB) and $\delta^{15}N$ in ‰ *vs.* air was lower than ±0.3‰. The chlorin index (CI) and total chlorin concentration were determined with an analytical precision of ±5% according to Schubert *et al.*[25]

2.5 Accumulation rates

Whereas the SR only includes linear sedimentation in a specific core, bulk accumulation rates (AR_{bulk}) also take compaction into account and hence sediment accumulation per time and area could be estimated. We used the following formulae:[21]

$$AR_{bulk} = SR \times \text{dry density} \times (1 - \text{porosity}/100) \quad (1)$$

$$AR_{TOC} = (TOC/100) \times AR\ \text{bulk} \quad (2)$$

where AR_{bulk} and AR_{TOC} (g cm^{-2} per year) are the accumulation rates of the bulk sediment and total organic carbon, respectively. Dry density (g cm^{-3}), SR (cm per year), porosity (%), and TOC (total organic carbon in %).

2.6 Lipid biomarker analysis

The sediment samples were extracted in methanol/dichloromethane using a microwave system (MLS) to obtain the total lipid extracts. Aliquots of the extracts were saponified after addition of internal standards and separated into fatty acid and neutral (non-saponifiable) lipid fractions. The neutral fractions were silylated (BSTFA, Sigma) and analyzed by gas chromatography and gas chromatography-mass spectrometry for the quantification and identification of biomarkers, respectively. For a detailed description of lipid extraction see ref. 26.

2.7 Methane concentrations

Sediment samples (2 cm^3) were taken from the sediment core by sub-sampling the sediment from the side of the plastic tube through pre-drilled holes that were covered by tape during sampling. The sediment was filled in a 20 mL glass vial with 4 mL of 1 M NaOH. Subsequently the glass was covered with a butyl stopper and sealed with an aluminum crimp. Dissolved CH_4 concentrations were measured in the headspace under controlled temperature conditions with an automated system (Joint Analytical Systems, Germany). In short, samples were introduced *via* an automated pumping system into a gas chromatograph (GC, Agilent) at constant temperature. The GC was equipped with a Carboxen 1010 column (30 m, Supelco) and a flame ionization detector. The oven temperature was 40 °C. CH_4 standards were prepared by dilution of pure CH_4 (99.9%) and calibrated against commercial references of 100 ppm, 1000 ppm and 1% (Scott, Supelco).

2.8 pH, alkalinity, and DIC

pH was measured on the boat within minutes following the retrieval of the peepers using a portable pH meter (model 704, Metrohm) and a glass electrode (Minitrode, Hamilton) calibrated with 2 buffer reference solutions (Merck) of pH 6 and 8. Alkalinity was determined by end-point titration using a titration device (Titrino, Metrohm) and hydrochloric acid (HCl, 0.01 M). Dissolved inorganic carbon (DIC) concentrations were estimated using the measurements of pH and alkalinity, and equilibrium constants at 20 °C.[27]

2.9 Stable isotopic composition of carbon in DIC ($\delta^{13}C_{DIC}$)

An aliquot of pore water was transferred without air bubbles onsite as fast as possible into a 2 mL glass vial, sealed with a Teflon cap using a crimper and kept at 4 °C. Before analysis, 1.5 mL of the water sample was transferred into an exetainer® and the headspace was flushed with helium. Concentrated phosphoric acid was added to convert all DIC to CO_2. 100 μL of headspace was withdrawn from the vials with a GasTight Hamilton syringe and injected into a GC (Hewlet Packard 5890) interfaced to a ConFlo IV and a Delta V Plus IRMS (Thermo Fisher Scientific, Bremen, Germany). The GC was equipped with a GS-Carboplot column (Agilent, 30 m × 0.32 mm × 1.5 micron) to separate CO_2 from the interfering gases.

2.10 Oxygen concentrations

Oxygen at the sediment–water interface was measured within an hour after the sampling. An oxygen micro-optode operated with a temperature compensated system (Microx TX3, PreSens) and a custom made step motor with a vertical resolution of 0.05 mm was used. The micro-optode was calibrated with oxygen-free and air saturated solutions. The oxygen-free calibration solution was prepared by dissolving 1 g of sodium sulfite (Na_2SO_3) in 100 mL of nanopure water and the air saturated calibration solution was prepared by purging with air for 20 minutes using a glass frit following the recommendations of the manufacturer. The micro-optode was positioned in the water overlying the sediments, and slowly brought close to the sediment–water interface until the oxygen values (% air saturation) decreased. From this point on, the oxygen values (% air saturation) were recorded with a vertical resolution of 0.05 to 0.1 mm with an equilibration time between measurements of 20 s. Oxygen was measured until values of 0% air saturation were obtained two times in a row. Up to nine oxygen profiles per site were recorded.

2.11 Determination of ammonium, sulfate, nitrate, iron and manganese

NH_4^+ concentrations were determined within hours following the sampling, using a standard photometric method following the protocol of GSM, 2002 (DIN 38 406-E5). Pore water aliquots were kept frozen until analysis of SO_4^{2-} and NO_3^- concentrations by ion chromatography (ICS 1000 Ion Chromatography System, Dionex). For Fe(II) and Mn(II) concentrations, pore water aliquots (2 mL) were acidified onsite with 45 μL ultrapure concentrated nitric acid (65%, VWR) within minutes after sampling and then kept frozen until analysis using inductively coupled plasma optical emission spectroscopy (ICP-OES, Spectro Analytical Instruments). Samples were diluted 25 and 125 times (pore water samples from the center of the lake and from the delta region, respectively).

2.12 Data analysis and calculation of mineralization rates

Areal fluxes across the sediment–water interface from sediment pore water data were determined with a model considering diffusion and reaction of dissolved compounds.[28] The model was fitted to measured pore water concentration profiles by adjustment of reaction rates. The concentration change, dC, of a compound at depth z below the sediment–water interface with time dt is:

$$\frac{\partial C(z,t)}{\partial (t)} = D_s \frac{\partial^2 C(z,t)}{\partial z^2} + \sum R(z) \quad (3)$$

and depends on the diffusion coefficient of the compound in the sediment, D_s, and the sum of process rates affecting the compound, $\Sigma R(z)$. We introduced two sediment layers with different reaction rates that allow accounting for easily degradable (R_1) and more refractory (R_2) organic matter, hence for the upper layer $\Sigma R(z) = -(R_1 + R_2)$ and for the lower layer $\Sigma R(z) = -R_2$.

The mathematics of the model are detailed in Epping and Helder (1997).[29] Diffusion coefficients at 4 °C were taken from Li and Gregory (1974).[30] The porosity of the sediment (ϕ) was measured and the resulting formation factor ($F = 1.02 \times \phi^{-1.81} = 1.23$) was used as suggested by Maerki *et al.* (2004).[31]

3 Results and discussion

The two regions chosen for our investigation showed clear quantitative differences in the measured parameters. Sedimentation rates of the two cores close to the river mouth were much higher (SR = 2.3 cm per year) than the ones in the deeper part of the lake (SR = 0.4–0.6 cm per year). This already showed that sites on the Rhone River delta received more particulate material than the ones further out in the lake. The ARs amount to 26.8 and 28.4 kg m^{-2} per year at sites #1 and #2, and to 4.1 and 2.4 kg m^{-2} per year at sites #4 and #5 (Table 1). The values from the delta are in the range of published values in front of the Rhone river of 45.9 kg m^{-2} per year.[32] The lowest OC contents (0.3–0.6%, Fig. 1) as a result of dilution by mineral particles delivered by the Rhone River were found at site #2, which together with site #1 is located closest to the river entrance. High OC values of ~1% and up to 1.35% in the deeper sediment were detected at site #5, the core furthest away from the delta. This resulted in an AR_{TOC} of 131.7 and 129.8 gC m^{-2} per year (sites #1 and #2) and 31.2 and 19.8 gC m^{-2} per year (sites #4 and #5), respectively for the delta and profundal sites (Table 1).

C/N ratios are a way to characterize the OM as autochthonous, *i.e.* locally produced in the lake, and allochthonous, *i.e.* originating from outside the aquatic system. Autochthonous OM consists of algae and bacteria and hence is rich in N (proteins), whereas terrestrial OM (leaves, grass, *etc.*) is depleted in N and enriched in O-containing compounds (*e.g.* lignins).[33] Therefore, C/N values for aquatic plants lie between 4 and 10, whereas terrestrial vascular plants can have values >20.[34] In this study C/N ratios decreased continuously from 10.1 close to the river mouth to 9.1 and 7.9, and finally 7.4 at the most profundal site #5 (Table 2). Although TOC contents increased towards the open lake due to decreasing dilution by mineral particles transported by the river, the increase of N was even higher leading to lower C/N ratios. C/N ratios (Table 2) indicated a higher terrestrial influence at the delta sites contrary to the deeper sites where autochthonous OM was prevalent.

The carbon isotopic composition of the OM ($\delta^{13}C_{org}$ values) is used frequently in the marine environment to distinguish marine from terrestrial OM.[35] However, in lacustrine systems the $\delta^{13}C_{org}$ values of those two sources are rather indistinguishable since autochthonously produced OM is isotopically very similar to terrestrial OM. The reason is that the $\delta^{13}C_{DIC}$ in lakes in general and in the water column of Lake Geneva in particular is already very depleted (around −10 to −15‰, see the uppermost peeper values in Fig. 2), which leads to isotopically very light autochthonous OM compared to marine plankton. Carbon isotope values of OM in sediments of Lake Geneva were between −24.8 and −29.0‰ (Fig. 1) and hence were difficult to interpret with respect to differentiation of the

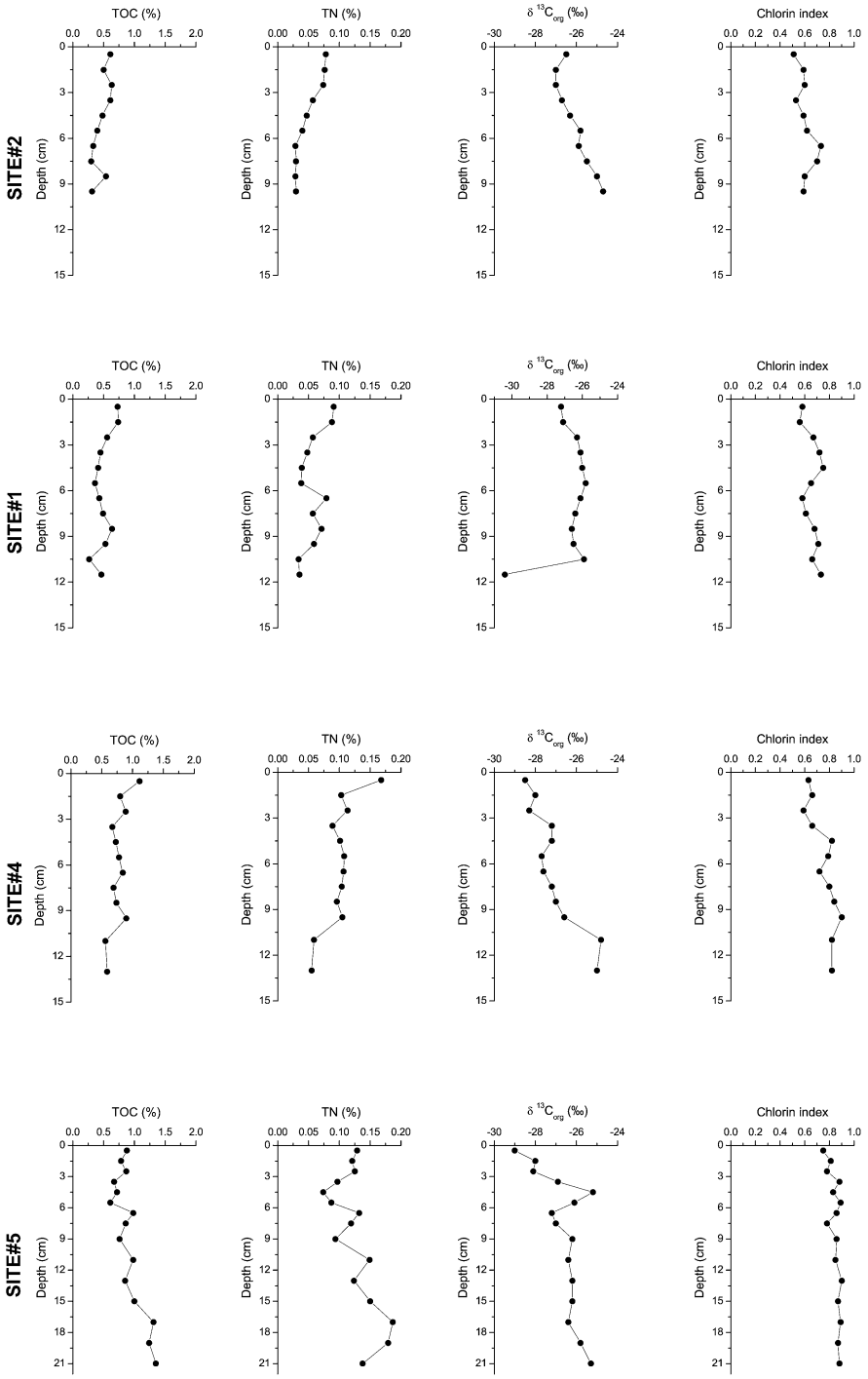

Fig. 1 Total organic carbon (TOC) and total nitrogen (TN) concentrations, the carbon isotopic composition of the OM ($^{13}C_{org}$), and the chlorin index (CI) of the sediments at sites #2, #1, #4, and #5.

OM as mentioned above. Nevertheless, our $\delta^{13}C_{org}$ results showed that OM isotopically was increasingly heavier towards the bottom of the cores indicating the more labile character of the isotopically light aquatic OM. Based on this finding one could argue that values above $-28‰$ are indicative of a more autochthonous material since these values are unusual for an allochthonous material and hence the profundal cores have a higher contribution of autochthonous, *i.e.*, algal material.

One parameter used quite frequently in sediments is the chlorin index (CI) together with chlorin concentrations.[25,36] Whereas the chlorin concentration gives a measure of how much pigment related OM is present in a sediment sample, the CI indicates how refractory is the OM. Relatively fresh OM has CI values of ~0.6 (fresh chlorophyll has a value of 0.2), whereas more degraded OM shows values between 0.8 and 1.0. The sediments of Lake Geneva showed CI values between 0.5 and 0.9

Table 2 Areal fluxes in [mmol m^{-2} d^{-1}] across the sediment–water interface in the Rhone River delta estimated from sediment pore water measurements. The mineralization rates (R) are in [mmol m^{-2} d^{-1}]

Parameter	Site 1	Site 2	Site 4	Site 5
O_2	4.3 ± 0.8 (n = 9)	4.1 ± 1.1 (n = 6)	8.2 ± 1.2 (n = 3)	8.8 ± 1.3 (n = 2)
NO_3^-	Nd	0.036	0.06	0.10
SO_4^{2-}	0.32	0.15	0.62	0.54
CH_4	1.96	2.34	0.69	0.50
NH_4^+	0.31	0.14	0.16	0.13
Fe(II)	1.1×10^{-4}	9.0×10^{-5}	3.8×10^{-4}	3.3×10^{-4}
Mn(II)	4.3×10^{-4}	9.2×10^{-4}	2.7×10^{-3}	7.6×10^{-3}
C/N ratio	10.1	9.1	7.9	7.4
$R_{aerobic}$	0.3 (6%)	0 (0%)	6.8 (72%)	7.8 (78%)
$R_{anaerobic}$	4.6 (94%)	5.0 (100%)	2.7 (28%)	2.2 (22%)
R_{total}	4.9 (100%)	5.0 (100%)	9.5 (100%)	10.0 (100%)

with lower values on the delta and higher values at the distant sites #4 and #5 (Fig. 1). Hence, the material closer to the river mouth was fresher than the material deposited far away from the river mouth. Chlorin concentrations normalized to TOC, however, were higher for the distant sites #4 and #5 with 1226 and 1358 μg g^{-1} TOC compared to the delta sites #1 and #2 with 1032 and 822 μg g^{-1} TOC. Combined we see higher amounts of degraded pigment material in the distant sites.

Further characterization of OM in terms of autochthonous *vs.* allochthonous sources was done using lipids.[34,37–39] Especially long chain *n*-alkanes and alcohols have been used as indicators for terrestrial OM. These compounds are constituents of surface waxes covering the leaves of higher plants.[40] The sum of the long chain *n*-alkanes (C_{27}, C_{29}, C_{31}) and long-chain alcohols (C_{24}, C_{26}, C_{28}) was calculated. The *n*-alkanes showed contents of 277 to 429 μg per gC (#1 and #2) and 126 to 175 μg per gC (#4 and #5) with around 2 times higher concentrations closer to the river mouth. Similar results were obtained for the long-chain alcohols with 804 to 1128 μg per gC and 368 to 538 μg per gC, respectively. Calculating the AR for long chain *n*-alkanes and alcohols revealed an even more drastic difference and showed that the deltaic sites received 6 to 25 (*n*-alkanes) and 8–16 (alcohols) times more terrestrial OC than the profundal sites. In conclusion, a higher terrestrial input prevailed towards the river mouth supporting the above interpretation based on C/N ratios.

The final products of OM degradation are CH_4 and CO_2 (quantified as DIC dissolved in the pore water, neglecting the DIC produced by calcite dissolution in the sediment). Both constituents were released from Lake Geneva sediments into the water column, as suggested by the shape of their concentration profiles (Fig. 2), which decreased towards the sediment surface. CH_4 fluxes varied spatially and were more intense in the river delta (1.96 and 2.34 at sites #2 and #1) compared to the deeper part of the lake (0.69 and 0.50 at sites #4 and #5, Table 2). The DIC fluxes were 2.0 and 1.4 mmol m^{-2} d^{-1} at sites #1 and #2 and 1.0 and 0.9 mmol m^{-2} d^{-1} at sites #4 and #5, respectively. Although DIC fluxes at the deltaic sites were not 4 to 5 times higher than those at the profundal sites, as was observed for CH_4, they were still 1.5 to 2 times higher hinting to more pronounced fluxes of the degradation products of OM at the deltaic sites.

The main focus of this study was to investigate the difference in electron acceptors used for the degradation of OM depending on its concentration and origin, *i.e.* lacustrine or terrestrial, in a lacustrine system. Hence, fluxes of O_2, SO_4, and NO_3 were calculated from the concentration profiles determined from peepers and sediment cores (Fig. 3, O_2 concentration profiles not shown but up to 9 profiles per site were combined to estimate fluxes).

The O_2 consumption of the sediment was similar for the profundal cores with 8.8 (site #4) and 8.2 mmol m^{-2} d^{-1} (site #5), whereas only half of this flux was measured at sites #1 and #2 close to the river inflow with 4.3 and 4.1 mmol m^{-2} d^{-1}, respectively (Table 2). O_2 concentrations in the deep waters were around 4 mg L^{-1} during the time of sampling (The Commission Internationale pour la Protection des Eaux du Léman, CIPEL). As described before for lacustrine sediments[12] O_2 penetrated only the uppermost mm of the sediment with the deepest penetration of 1.8 mm at site #1. The other two electron acceptors NO_3^- and SO_4^{2-} showed very small fluxes compared to O_2. The NO_3^- flux could not be determined at site #1 due the large scatter of the data. At site #2 the NO_3^- flux was lower (0.04 mmol m^{-2} d^{-1}) than that at the deeper sites #4 and #5 where 0.06 and 0.1 mmol m^{-2} d^{-1} were measured. Similarly, the SO_4^{2-} flux into the sediment was lower at the shallower sites #1 and #2 (0.15 and 0.32 mmol m^{-2} d^{-1}) than that at the deeper sites #4 and #5 (0.62 and 0.54 mmol m^{-2} d^{-1}).

The fluxes of reduced species from the sediments (Table 2) decreased from the delta to the sites in the open lake for CH_4 (from 2.3 to 0.5 mmol m^{-2} d^{-1}) and NH_4^+ (from 0.31 to 0.13 mmol m^{-2} d^{-1}). Fluxes of Fe(II) and Mn(II), however, increased although they were generally very low (between 9×10^{-5} and 7.6 $\times$ 10^{-3} mmol m^{-2} d^{-1}). The CH_4 fluxes were comparable to values reported by Sollberger *et al.* (2014)[41] who showed that diffusive CH_4 fluxes were more intense in the active canyon of the Rhone delta than in the central and eastern regions. The sites with lower OC concentrations (sites #1 and #2) had higher

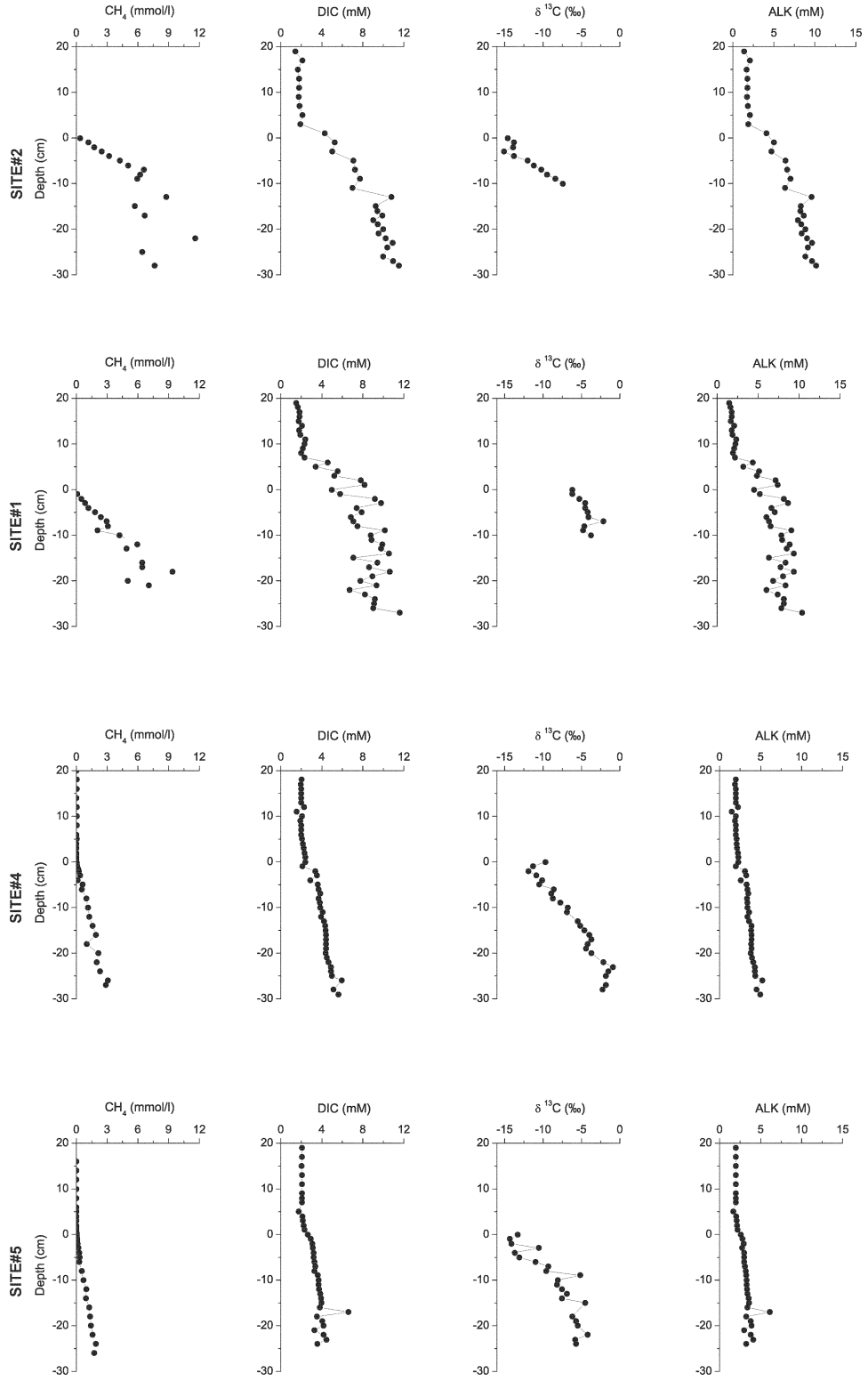

Fig. 2 Methane (CH_4) and dissolved inorganic carbon (DIC) concentrations in the pore waters of the four sediment cores, the carbon isotopic composition of the DIC ($^{13}C_{DIC}$), and the alkalinity (ALK) at the four sites.

CH_4 fluxes, whereas sites #4 and #5 comprised higher OC contents but lower CH_4 fluxes. However, one has to take into account that the AR of OC was about five times higher at the delta sites than that at the deep sites and the low content is a 'dilution' by non organic, *i.e.* minerals, delivered by the river.

If the production rate of CH_4 is related to the deposition rate of OC we receive an efficiency for the methanogenesis from total

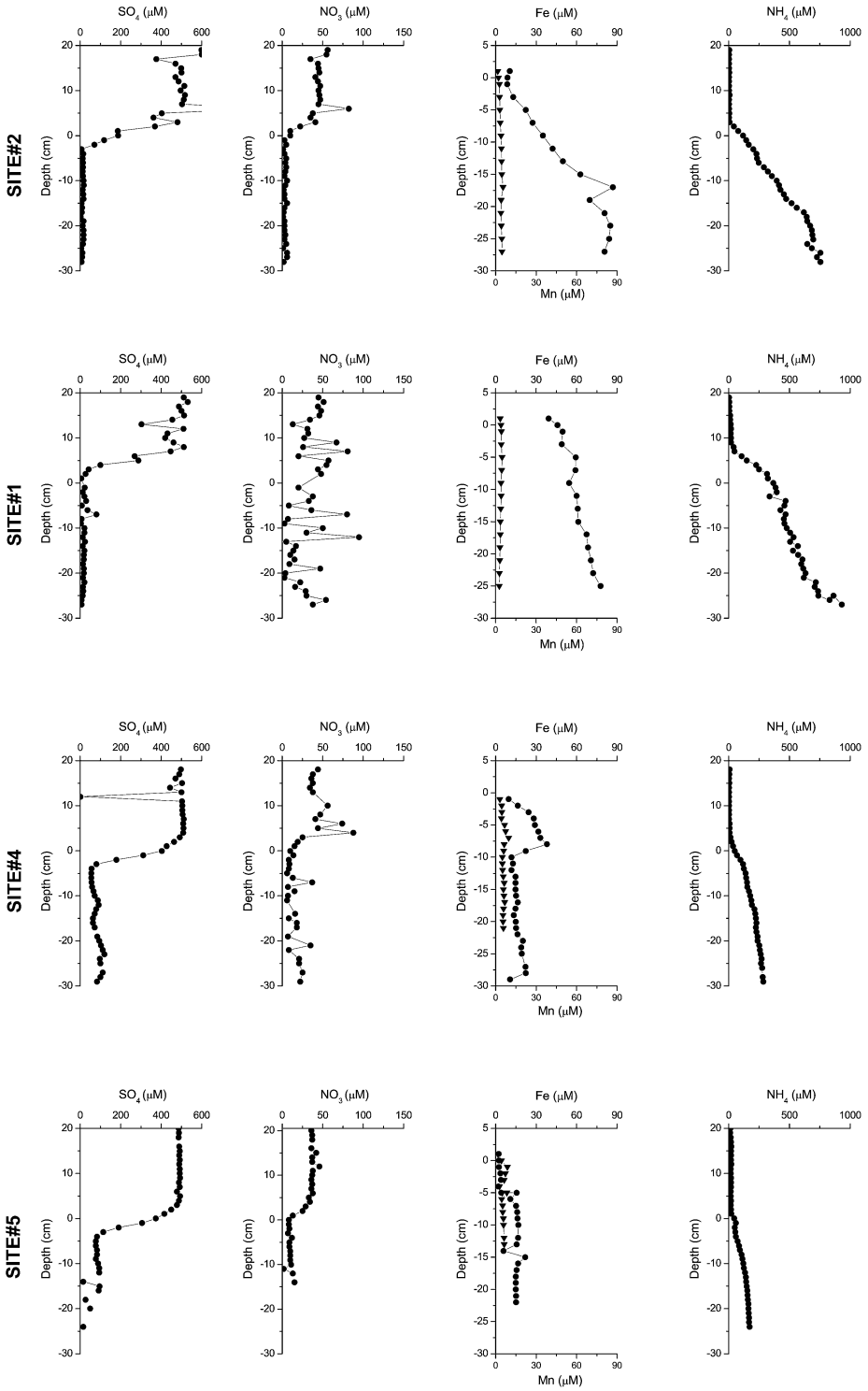

Fig. 3 Concentrations of sulfate, nitrate, manganese (triangles), iron (circles), and ammonium measured in the pore water and overlaying water of the sites #1, #2, #4, and #5.

OC (in mmol CH_4 per gC) that is now clearly higher at the deeper sites than in the delta (Table 1). Hence, it seems that the AR_{OC} is not solely responsible for the degree of CH_4 production, but that beside the accumulation of OC additional parameters like freshness/degradability and composition of the OM play a role.

The set of available pore water data allowed estimating the mineralization rates of OM R_{total} at the four sites, and the fraction of OM degraded aerobically ($R_{aerobic}$) and anaerobically ($R_{anaerobic}$). As exemplified by Maerki *et al.* (2009)[12] oxic mineralization was calculated from the flux of O_2 to the sediment

subtracting reduced compounds diffusing up from the deeper sediments thus contributing to the consumption of O_2:

$$R_{\text{aerobic}} = J_{O_2} - 2 \times J_{CH_4} - 0.5 \times J_{Mn(II)} - 0.25 \times J_{Fe(II)} \quad (4)$$

The stoichiometric factors define the equivalents of O_2 consumed per equivalent of reduced compounds. The areal mineralization of OM is expressed in mmol C m^{-2} d^{-1} (Table 2) assuming the mineralization of one equivalent of OM per equivalent of O_2, thus neglecting nitrification. The fraction of OM mineralized with electron acceptors other than O_2 ($R_{\text{anaerobic}}$) is calculated as:

$$R_{\text{anaerobic}} = 1.25 \times J_{NO_3^-} + 0.25 \times J_{Fe(II)} + 0.5 \times J_{Mn(II)} + 2 \times J_{SO_4^{2-}} + 2 \times J_{CH_4} \quad (5)$$

Since we could not account for compounds that were potentially removed from the pore water and buried such as precipitates of Fe(II)/Mn(II) sulfides, vivianite, siderite, *etc.*, those sinks were neglected.

The rates for totally mineralized OM ($R_{\text{total}} = R_{\text{aerobic}} + R_{\text{anaerobic}}$) presented in Table 2 at the deeper sites #4 and #5 (average of 9.7 mmol C m^{-2} d^{-1}) were two times higher than those at the shallower sites #1 and #2 (4.7 mmol C m^{-2} d^{-1}). Not only the rates were different but also the mineralization pathway differed between the shallow sites #1 and #2 in the Rhone River delta, and the profundal sites #4 and #5. Only 0–6% was mineralized aerobically at the shallow sites, since almost all O_2 was used to oxidize the large flux of CH_4 from below (Fig. 4). At the deeper sites, the situation was reversed and the fraction of aerobically degraded OM was between 72 and 78% (Fig. 4). Also, the contribution of SO_4^{2-} to $R_{\text{anaerobic}}$ was very distinct between both areas with 44–49% at the deeper sites and only 6–14% at the shallower sites. The contributions of NO_3^- (1–5.5%), and of Fe and Mn (<0.2%) to the mineralization of OM in the sediments were negligible.

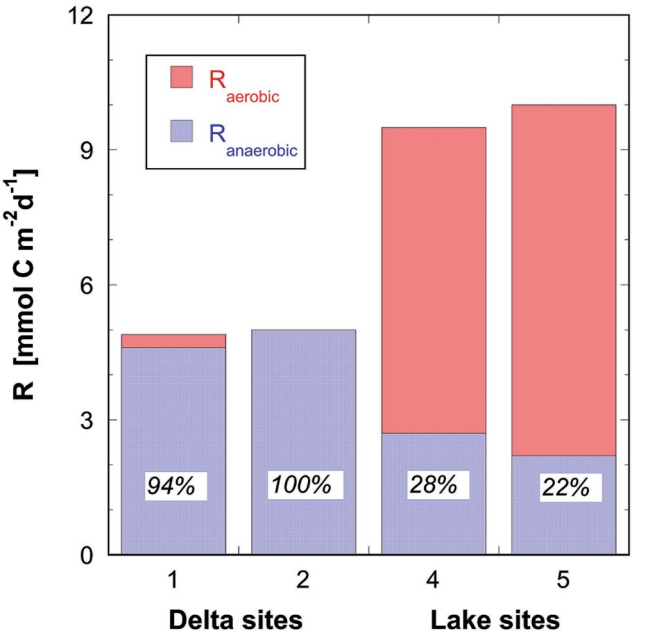

Fig. 4 Aerobic and anaerobic degradation rates of the river delta sites and of the profundal sites. Whereas sites #1 and #2 show a degradation that is mainly triggered by anaerobic degradation (94 and 100%), sites #4 and #5 show a dominance of aerobic degradation with an anaerobic fraction of only 28 and 22%.

The increased generation of alkalinity observed in the sediment pore water of the shallow sites (Fig. 2) lessens up to 10% by the dissolution of calcite (determined from Ca^{2+} pore water profiles, data not shown), and even less at the deeper sites. However, the reduction of SO_4^{2-} with both, OM or CH_4 produces one equivalent of alkalinity, which for sites 1 and 2 amounts to 11–16% of the HCO^{3-} flux but to ~60% for sites 4 and 5. Similarly, alkalinity generated by denitrification is ~3% at site 2, but 6–11% at sites #4 and #5. Contributions from Fe and Mn reduction are negligible. The remaining HCO^{3-} originates from the production of CO_2 by mineralization and the subsequent decrease of pH.

In conclusion, a consistent picture emerged that the mineralization pathways and rates in the sedimentary depositions in the Rhone delta area were significantly different from those out in the profundal parts of the lake. The much higher CH_4 fluxes in the delta compared to the open lake sites are explained by the high deposition rate of OC in this area where OC accumulation was approximately 5 times higher in the delta at sites #1 and #2 (132 and 130 gC m^{-2} per year) than at sites #4 and #5 (31.2 and 19.8 gC m^{-2} per year, Table 1). Bulk deposition rates differed even by a factor of 8 (Table 1) demonstrating the high load of mineral particles transported by the river and diluting the OC. These "diluting" conditions led to almost two times higher content of OC (in percent %) at the profundal than at the delta sites. Estimating the efficiency of CH_4 formation per equivalent of OC (the annual flux of CH_4 per annually deposited C) therefore resulted in 5.5 to 6.4 μmol CH_4 per gC and of 8.0 to 9.1 μmol CH_4 per gC for the delta sites and open lake sites, respectively (Table 1). This supports our findings that a significant part of the OC deposited in the delta contained more refractory and thus microbially less degradable, terrestrial material. The higher CH_4 flux on the delta must be recognized as caused by the high AR and the small fraction of aerobic mineralization of OC, which was qualitatively different from the more autochthonous material at the deeper sites and thus could be converted to CH_4 only with a lower efficiency. This study supports earlier findings that have claimed that burial in lakes is high[9] and it is especially high when high amounts of allochthonous material are delivered.[4] It also points out that it is necessary not only to measure the OM concentration but to characterize the origin and the degradation state of OM to estimate how OM is transformed and which share is emitted as CO_2 and/or CH_4.

Similar to river deltas in the coastal ocean, river deltas of large lakes are active players in the carbon cycle as OM is buried, transformed or emitted from bottom sediments. However, an accurate estimate of the amount of carbon cycled in these active zones remains relatively unconstrained, largely because the fractions of various carbon sources are unresolved. Our results suggest that carbon sources and

degradation pathways can differ widely in some freshwater systems, further complicating the situation. While similar analyses as those presented here would be necessary to accurately identify OC sources and degradation pathways, the clear trends in our data indicate that river deltas are regions of substantial carbon cycling, and that any system resembling our study site, particularly if it is an obvious hot spot for CH_4 production (*i.e.*, presence of ebullition), will exhibit the same redox conditions and OM degradation patterns we observed in the Rhone delta.

Acknowledgements

This publication is part of the international, interdisciplinary research project éLEMO for the investigation of the deep-waters of Lake Geneva using two Russian MIR submarines (http://www.elemo.ch). Funding for retrieving samples was provided by the ''Fondation pour l'Etude des Eaux du Léman'' (FEEL; in particular by the Ferring Pharmaceuticals, St. Prex). Laboratory and personnel was funded by Eawag. We thank the Russian MIR crew members (http://www.elemo.ch/mir-team) for their excellent performance and the SAGRAVE team who provided and operated the platform from which the dives were carried out. We also thank Ulrich Lemmin and Jean-Denis Bourquin for project coordination. The service of Mikhail Kranoperov (Russian Honorary Consulate) as liaison is greatly appreciated. We also thank C. Dinkel, M. Schurter, and A. Zwyssig for fieldwork assistance. R. Stierli and late G. Nobbe are thanked for the lab assistance. The Commission Internationale pour la Protection des Eaux du Léman (CIPEL) is thanked for providing O_2 concentrations in the bottom water of Lake Geneva. Finally we thank all scientists of the éLEMO project for the excellent collaboration and two reviewers who really helped to improve this manuscript.

Notes and references

1 J. I. Hedges and R. G. Keil, *Mar. Chem.*, 1995, **49**, 81–115.
2 H. E. Hartnett, R. G. Keil, J. I. Hedges and A. H. Devol, *Nature*, 1998, **391**, 572–575.
3 D. J. Burdige, *Chem. Rev.*, 2007, **107**, 467–485.
4 S. Sobek, E. Durisch-Kaiser, R. Zurbrugg, N. Wongfun, M. Wessels, N. Pasche and B. Wehrli, *Limnol. Oceanogr.*, 2009, **54**, 2243–2254.
5 S. Sobek, R. Zurbrugg and I. Ostrovsky, *Aquat. Sci.*, 2011, **73**, 355–364.
6 J. Chappellaz, J. Barnola, D. Raynaud, Y. Korotkevich and C. Lorius, *Nature*, 1990, **345**, 127–135.
7 *Climate Change. The IPCC Scientific Assessment*, ed. J. T. Houghton, G. J. Jenkins and J. J. Ephraums, Cambridge University Press, Cambridge, 1990.
8 D. J. Wuebbles and K. Hayhoe, *Earth-Sci. Rev.*, 2002, **57**, 177–210.
9 W. E. Dean and E. Gorham, *Geology*, 1998, **26**, 535–538.
10 J. A. Downing, Y. T. Prairie, J. J. Cole, C. M. Duarte, L. J. Tranvik, R. G. Striegl, W. H. McDowell, P. Kortelainen, N. F. Caraco, J. M. Melack and J. J. Middelburg, *Limnol. Oceanogr.*, 2006, **51**, 2388–2397.
11 D. E. Canfield, B. B. Jorgensen, H. Fossing, R. Glud, J. Gundersen, N. B. Ramsing, B. Thamdrup, J. W. Hansen, L. P. Nielsen and P. O. J. Hall, *Mar. Geol.*, 1993, **113**, 27–40.
12 M. Maerki, B. Mueller, C. Dinkel and B. Wehrli, *Limnol. Oceanogr.*, 2009, **54**, 428–438.
13 P. Burkard, in *Lausanne: Le Léman Synthèse 1957–1982*, 1984, pp. 43–48.
14 OFEV, *Annuaire hydrologique de la Suisse 2009*, Office fédéral de l'environnement, Berne, Switzerland, 2013, p. 617.
15 D. Burrus, R. Thomas, J. Dominik and J. Vernet, *Hydrol. Processes*, 1989, 65–74.
16 N. R. Urban, C. Dinkel and B. Wehrli, *Aquat. Sci.*, 1997, **59**, 1–25.
17 S. Girardclos, M. Hilbe, J. P. Corella, J. L. Loizeau, K. Kremer, T. Delsontro, A. Arantegui, A. Moscariello, F. Arlaud, Y. Akhtman, F. S. Anselmetti and U. Lemmin, *Arch. Sci.*, 2012, **65**, 103–118.
18 R. H. Hesslein, *Limnol. Oceanogr.*, 1976, **21**, 912–914.
19 H. Brandl and K. W. Hanselmann, *Aquat. Sci.*, 1991, **53**, 55–73.
20 R. Carignan, S. S. Pierre and R. Gachter, *Limnol. Oceanogr.*, 1994, **39**, 468–474.
21 F. Niessen, L. Wick, G. Bonani, C. Chondrogianni and C. Siegenthaler, *Aquat. Sci.*, 1992, **54**, 257–276.
22 P. G. Appleby and F. Oldfield, *Catena*, 1978, **5**, 1–8.
23 J. P. Corella, A. Arantegui, J. L. Loizeau, T. DelSontro, N. le Dantec, N. Stark, F. S. Anselmetti and S. Girardclos, *Aquat. Sci.*, 2014, **76**(suppl. 1), 73–87.
24 C. J. Schubert and B. Nielsen, *Mar. Chem.*, 2000, **72**, 55–59.
25 C. J. Schubert, J. Niggemann, G. Klockgether and T. G. Ferdelman, *Geochem., Geophys., Geosyst.*, 2005, **6**, 1–12.
26 S. Naeher, R. H. Smittenberg, A. Gilli, E. P. Kirilova, A. F. Lotter and C. J. Schubert, *Org. Geochem.*, 2012, **49**, 86–95.
27 W. Stumm and J. J. Morgan, *Aquatic Chemistry, An Introduction Emphasizing Chemical Equilibria in Natural Waters*, Wiley, J., New York, 1981.
28 B. Müller, Y. Wang, M. Dittrich and B. Wehrli, *Water Res.*, 2003, **37**, 4524–4532.
29 E. H. G. Epping and W. Helder, *Cont. Shelf Res.*, 1997, **17**, 1737–1764.
30 Y. H. Li and S. Gregory, *Geochim. Cosmochim. Acta*, 1974, **38**, 703–714.
31 M. Maerki, B. Wehrli, C. Dinkel and B. Müller, *Geochim. Cosmochim. Acta*, 2004, **68**, 1519–1528.
32 J.-L. Loizeau, *Arch. Sci.*, 1998, **51**, 13–25.
33 J. I. Hedges, W. A. Clark, P. D. Quay, J. E. Richey, A. H. Devol and U. d. M. Santos, *Limnol. Oceanogr.*, 1986, **31**, 717–738.
34 P. A. Meyers and R. Ishiwatari, *Org. Geochem.*, 1993, **20**, 867–900.
35 C. J. Schubert and S. E. Calvert, *Deep Sea Res., Part I*, 2001, **48**, 789–810.
36 A. N. Meckler, C. J. Schubert, G. L. Cowie, S. Peiffer and M. Dittrich, *Limnol. Oceanogr.*, 2004, **49**, 2023–2033.

37 L. Westerhausen, J. Poynter, G. Eglinton, H. Erlenkeuser and M. Sarnthein, *Deep-Sea Res.*, 1992, 1–53, in press.
38 C. J. Schubert and R. Stein, *Org. Geochem.*, 1996, **24**, 421–436.
39 S. Bourgeois, A. M. Pruski, M. Y. Sun, R. Buscail, F. Lantoine, P. Kerhervé, G. Vétion, B. Rivière and F. Charles, *Biogeosciences*, 2011, **8**, 3107–3125.
40 G. Eglinton and R. J. Hamilton, *Science*, 1967, **156**, 1322–1335.
41 S. Sollberger, J. P. Corella, S. Girardclos, M. E. Randlett, C. J. Schubert, D. B. Senn, B. Wehrli and T. DelSontro, *Aquat. Sci.*, 2014, **76**(suppl. 1), S89–S101.